

Influence of GaAs substrate on the transmission performance of epitaxially grown Fabry-Pérot filter

Wei Wang (王伟)*, Yongqing Huang (黄永清), Xiaofeng Duan (段晓峰), Qiang Yan (颜强), Xiaomin Ren (任晓敏), Shiwei Cai (蔡世伟), Jingwei Guo (郭经纬), and Hui Huang (黄辉)

State Key Laboratory of Information Photonics and Optical Communications, Ministry of Education, Beijing University of Posts and Telecommunications, Beijing 100876, China

*Corresponding author: wwaz2001@163.com

Received March 3, 2011; accepted May 9, 2011; posted online July 29, 2011

The influence of GaAs substrate on the transmission performance of a multi-film Fabry-Pérot filter (FPF), fabricated by metalorganic chemical vapor deposition epitaxial growth on GaAs substrate, is investigated using the transfer matrix method. On the basis of the theoretical simulation, we determine that the quality of the resonant transmission peak of this epitaxially grown FPF (EG-FPF) deteriorates through splitting when the substrate is taken into account. Rapid periodic oscillation of peak-transmittivity along with the alteration of substrate thickness is also observed in the simulation results. Finally, a remarkably improved transmission performance of the EG-FPF is obtained by thinning the substrate down to a suitable thickness range through well-controlled grinding and polishing.

OCIS codes: 130.3130, 230.1480, 230.7408.

doi: 10.3788/COL201109.111301.

Fabry-Pérot filters (FPFs) have been investigated in various microstructural systems for the past few decades^[1–4]. Along with the development of technologies and techniques such as metalorganic chemical vapor deposition (MOCVD) and molecular beam epitaxy, depositing high-quality epitaxial thin films onto different kinds of substrates using various materials has become possible^[5–7]. Thus, researchers introduced a kind of epitaxially grown FPF (EG-FPF) consisting of distributed Bragg reflectors (DBRs) of quarter-wave-stack on semiconductor substrate; promising special functions were achieved in these investigations^[8–11]. Furthermore, the transmission performance of the filter is one of its most important properties. However, regardless of the existence of substrates, most researchers continue to investigate EG-FPF transmission performance only under ideal cases^[8–11]. Such an approach imposes critical restrictions on performance improvements in relative devices. Hums *et al.* discussed the substrate effect in their paper^[12]. The current work differs intrinsically from theirs in that we concentrate on the modulation effect of the lower substrate, whereas they focus on the multimode effect of the upper Fabry-Pérot (F-P) cavity. In this letter, we primarily investigate semiconductor substrate influence on the transmission performance of EG-FPF.

A GaAs wafer with a thickness of around 350 μm was chosen as the substrate. Considering the lattice matching and refractive index contrast between epitaxial thin films, the bottom and top DBRs of the EG-FPF were made with GaAs/AlGaAs alternate quarter-wave-stack^[13]. A schematic of the EG-FPF is shown in Fig. 1; the EG-FPF consists of, from top and bottom, in turn, k (a positive integral) pairs of GaAs/AlGaAs quarter-wave-stack at the bottom DBR, GaAs resonant cavity layer, and k pairs of AlGaAs/GaAs quarter-wave-stack at the top DBR. When it comes to periodic thin-film structures, the transfer matrix method is commonly used as it is regarded as a most powerful tool^[14,15]. If the GaAs layer

with a high refractive index and the AlGaAs layer with a low refractive index in the DBR are denoted by H and L, the refractive transfer matrices for a light wave travelling from H to L and vice versa can be given by \mathbf{M}_{HL} and \mathbf{M}_{LH} , respectively, as follows:

$$\mathbf{M}_{\text{LH}} = \frac{1}{2} \begin{pmatrix} 1 + n_{\text{H}}/n_{\text{L}} & 1 - n_{\text{H}}/n_{\text{L}} \\ 1 - n_{\text{H}}/n_{\text{L}} & 1 + n_{\text{H}}/n_{\text{L}} \end{pmatrix},$$

$$\mathbf{M}_{\text{HL}} = \frac{1}{2} \begin{pmatrix} 1 + n_{\text{L}}/n_{\text{H}} & 1 - n_{\text{L}}/n_{\text{H}} \\ 1 - n_{\text{L}}/n_{\text{H}} & 1 + n_{\text{L}}/n_{\text{H}} \end{pmatrix},$$
(1)

where n_{H} and n_{L} denote the refractive indices of the GaAs and AlGaAs layers, respectively. The phase transfer matrices in uniform regions H and L can be expressed by \mathbf{U}_{H} and \mathbf{U}_{L} as

$$\mathbf{U}_{\text{H}} = \begin{pmatrix} \exp(i2\pi\Lambda_{\text{H}}n_{\text{H}}/\lambda) & 0 \\ 0 & \exp(-i2\pi\Lambda_{\text{H}}n_{\text{H}}/\lambda) \end{pmatrix},$$

$$\mathbf{U}_{\text{L}} = \begin{pmatrix} \exp(i2\pi\Lambda_{\text{L}}n_{\text{L}}/\lambda) & 0 \\ 0 & \exp(-i2\pi\Lambda_{\text{L}}n_{\text{L}}/\lambda) \end{pmatrix},$$
(2)

where λ denotes the incident wavelength, and Λ_x is the thickness of uniform region x ($x = \text{H}, \text{L}$), equal to $\lambda_0/4n_x$, in which λ_0 is the designed resonant transmission peak wavelength. Then, using refractive transfer matrices Eq. (1) and phase transfer matrices Eq. (2), the transfer matrices for one

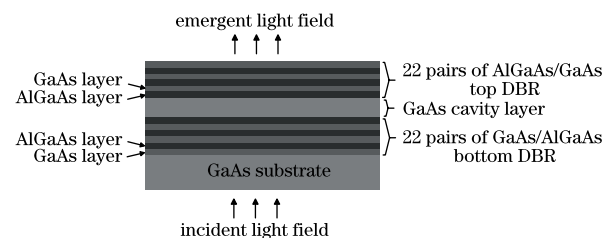


Fig. 1. Schematic of the EG-FPF on GaAs substrate.

period of the bottom DBR and one period of the top DBR can then be given by \mathbf{M}_B and \mathbf{M}_T , respectively, as follows:

$$\begin{aligned}\mathbf{M}_B &= \mathbf{U}_H \mathbf{M}_{HL} \mathbf{U}_L \mathbf{M}_{LH}, \\ \mathbf{M}_T &= \mathbf{M}_{HL} \mathbf{U}_L \mathbf{M}_{LH} \mathbf{U}_H.\end{aligned}\quad (3)$$

Assuming that both the incident and emergent media are air, the total transfer matrix of the EG-FPF can be given by

$$\begin{aligned}\mathbf{T} &= \frac{1}{2} \begin{pmatrix} 1 + n_H & 1 - n_H \\ 1 - n_H & 1 + n_H \end{pmatrix} \\ &\cdot \begin{pmatrix} \exp(i2\pi\Lambda_S n_H/\lambda) & 0 \\ 0 & \exp(-i2\pi\Lambda_S n_H/\lambda) \end{pmatrix} \\ &\cdot \mathbf{M}_B^k \begin{pmatrix} \exp(i2\pi\Lambda_C n_H/\lambda) & 0 \\ 0 & \exp(-i2\pi\Lambda_C n_H/\lambda) \end{pmatrix} \\ &\cdot \mathbf{M}_T^k \frac{1}{2} \begin{pmatrix} 1 + 1/n_H & 1 - 1/n_H \\ 1 - 1/n_H & 1 + 1/n_H \end{pmatrix} \\ &= \mathbf{M}_0 \mathbf{U}_S \mathbf{M}_B^k \mathbf{U}_C \mathbf{M}_T^k \mathbf{M}'_0 = \begin{pmatrix} \mathbf{T}_{11} & \mathbf{T}_{12} \\ \mathbf{T}_{21} & \mathbf{T}_{22} \end{pmatrix},\end{aligned}\quad (4)$$

where Λ_C , which should be the integral multiple of $\lambda_0/2n_H$, is the length of the EG-FPF cavity, Λ_S denotes the thickness of the substrate, \mathbf{U}_S and \mathbf{U}_C are the phase transfer matrices of the substrate and EG-FPF cavity layer, respectively, and \mathbf{M}_0 represents the refractive transfer matrix from air toward the filter, while \mathbf{M}'_0 describes an inverse case. From Eq. (4), we determine that the vertically incident light fields transmitted through the EG-FPF can be written as

$$\begin{pmatrix} \mathbf{E}_i^+ \\ \mathbf{E}_i^- \end{pmatrix} = \begin{pmatrix} \mathbf{T}_{11} & \mathbf{T}_{12} \\ \mathbf{T}_{21} & \mathbf{T}_{22} \end{pmatrix} \begin{pmatrix} \mathbf{E}_o^+ \\ \mathbf{E}_o^- \end{pmatrix},\quad (5)$$

where \mathbf{E}_i^+ and \mathbf{E}_i^- are the forward and backward light fields in the incident side, respectively, while \mathbf{E}_o^+ and \mathbf{E}_o^- are those in the emergent side. Given that $\mathbf{E}_o^- = 0$, disregarding the loss of light fields transmitted through the filter yields the total transmittivity \mathbf{T}_{F-P} of the EG-FPF, expressed as

$$\mathbf{T}_{F-P} = \frac{1}{\mathbf{T}_{11}} \cdot \frac{1}{\mathbf{T}_{11}^*} = \frac{1}{|\mathbf{T}_{11}|^2}.\quad (6)$$

Assume that designed transmission peak wavelength λ_0 is 1550 nm. To receive a transmission spectrum with an appropriate full width at half maximum (FWHM) around 1 nm, we set $n_H = 3.5256$, $n_L = 3.1637$, $k = 22$, and $\Lambda_C = 9\lambda_0/2n_H$, simultaneously. The EG-FPF can be separated into two parts: the upper DBR-based filter and the lower substrate. The upper filter possesses a high finesse of 190 because of the high reflectivity of the two DBR mirrors.

The ideal case is considered by disregarding the contribution of the GaAs substrate (i.e., $\Lambda_S = 0$), and a simulated transmission spectrum calculated from Eq. (6) is shown in Fig. 2(a). By taking the substrate into account, three substrate thickness values of $\Lambda_{S1} = 50.559 \mu\text{m}$, $\Lambda_{S2} = 202.235 \mu\text{m}$, and $\Lambda_{S3} = 343.799 \mu\text{m}$ are chosen to

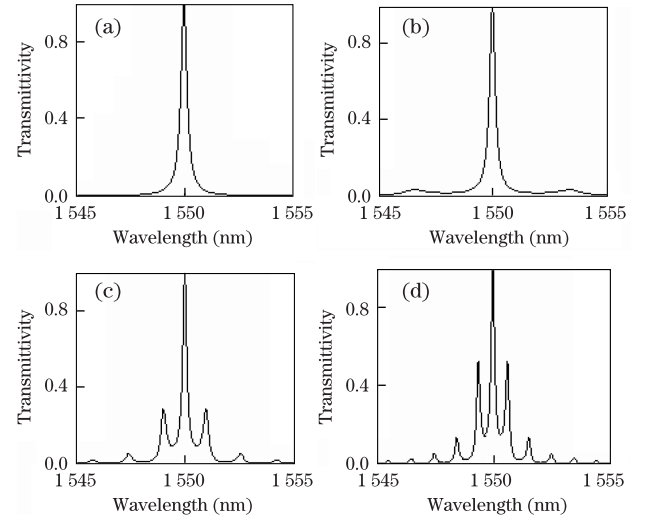


Fig. 2. Profiles of the simulated transmission spectra of the EG-FPF at substrate thicknesses of (a) $\Lambda_S = 0$, (b) $\Lambda_{S1} = 50.559 \mu\text{m}$, (c) $\Lambda_{S2} = 202.235 \mu\text{m}$, and (d) $\Lambda_{S3} = 343.799 \mu\text{m}$.

demonstrate the variation trend of the transmission performance of the EG-FPF via the alteration of substrate thickness. Λ_{S1} , Λ_{S2} , and Λ_{S3} are set to be the integral multiples of $\lambda_0/2n_H$.

Figure 2(a) displays a perfect transmission spectrum when $\Lambda_S = 0$. By contrast, the transmission peak begins to deteriorate through splitting as substrate thickness increases, as distinctly shown in Figs. 2(b)–(d). The thicker the substrate, the worse the transmission peak. When the substrate becomes thinner, on the other hand, the transmission spectrum exhibits an acceptable level to some extent (Fig. 2(b)), although a trend of side peaks occurs on both sides of the main transmission peak.

The substrate itself is also a kind of F-P cavity structure. However, its finesse is only about 1.9, resulting from the much lower reflectivity of its surface. The simulated transmission spectra of the substrate at Λ_{S1} , Λ_{S2} , and Λ_{S3} are shown in Figs. 3(a)–(c), respectively, which shows that the free spectrum range (FSR) of the fringes stemming from the substrate decreases in pace as substrate thickness increases. When the FSR diminishes over a certain range (e.g., the substrate is sufficiently thick), the transmission spectrum of the EG-FPF is significantly modulated by the substrate. This result is reasonable because when the FSR diminishes, the FWHM of the fringes stemming from the substrate also decreases ($\text{FWHM} = \text{FSR}/\text{finesse}$), so that these become comparable to the fringes stemming from the DBR filter. These fringes appear as side peaks in the observed output spectrum.

According to the analysis above, the splitting of the transmission spectra in Fig. 2 can be attributed to the periodic modulation of the substrate. The side peaks appearing in the measured response spectra of the devices in Refs. [9–11] must also be the contribution of the substrate.

The simulation result for the peak transmittivity (PT) of the EG-FPF as a function of substrate thickness is shown in Fig. 4. Rapid oscillation of the PT, along with a substrate thickness of 0–350 μm , is illustrated

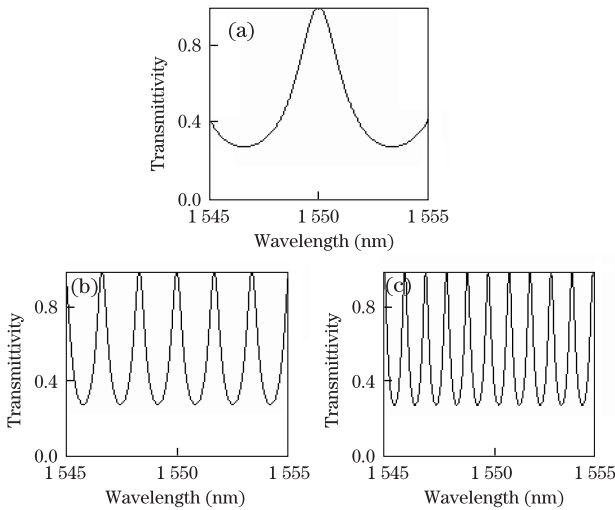


Fig. 3. Profiles of the simulated transmission spectra of the substrates at substrate thicknesses of (a) $A_{S1} = 50.559 \mu\text{m}$, (b) $A_{S2} = 202.235 \mu\text{m}$, and (c) $A_{S3} = 343.799 \mu\text{m}$.

in Fig. 4(a), which also exhibits that the oscillation amplitude of the PT increasingly strengthens along with the decrease in substrate thickness. Part of Fig. 4(a) is amplified and denoted as Fig. 4(b) to display the PT details, with the substrate thickness increasing from 0 to 1000 nm. The oscillation period of the PT is 220 nm (e.g., $\lambda_0/2n_H$). Thus, for the convenience of making comparisons, we set the values of substrate thickness as A_{S1} , A_{S2} , and A_{S3} to be the integral multiples of $\lambda_0/2n_H$ in Fig. 2.

When the substrate thickness equals $i\lambda_0/2n_H$ (i is a positive integral), constructive interference occurs within the substrate, which leads to a maximum EG-FPF transmittivity at 1550 nm. However, when the substrate thickness is $i\lambda_0/2n_H \pm \lambda_0/4n_H$, destructive interference occurs and yields a minimum transmittivity at 1550 nm. The difference between the two substrate thicknesses corresponding to successive constructive and destructive interferences is $\lambda_0/4n_H$. If the deviation of the substrate thickness from the ideal conditions of $i\lambda_0/2n_H$ is less than half of $\lambda_0/4n_H$ (e.g., $i\lambda_0/8n_H$), the PT is acceptable. Figure 4(b) shows that the PT is maintained at more than 0.9 if substrate thickness A_S is at the range given by

$$(i\lambda_0/2n_H - 55 \text{ nm}) < A_S < (i\lambda_0/2n_H + 55 \text{ nm}). \quad (7)$$

Considering $\lambda_0/8n_H \approx 55 \text{ nm}$, Eq. (7) can be rewritten as

$$(i\lambda_0/2n_H - \lambda_0/8n_H) < A_S < (i\lambda_0/2n_H + \lambda_0/8n_H). \quad (8)$$

Combining Figs. 2–4, we theoretically determine that the transmission spectrum of the EG-FPF splits because of the periodic modulation of the substrate. The thicker the substrate, the worse the transmission spectrum. To obtain an acceptable transmission spectrum, an alternative is to thin the substrate down to a suitable thickness (around $50 \mu\text{m}$ fitting to the design proposed in this letter) for the suppression of the side-peaks by well-controlled grinding and polishing; meanwhile, substrate thickness A_S should satisfy Eq. (8) to maintain the PT at more than 0.9.

Based on the parameters mentioned previously, an EG-FPF was fabricated by epitaxial growth on a $352\text{-}\mu\text{m}$ -thick GaAs wafer via MOCVD. Its cross-sectional scanning electron microscope (SEM) image is shown in Fig. 5(a). Then, three sub EG-FPFs with roughly the same area of around $0.5 \times 0.5 \text{ (cm)}$ were obtained through cleavage from the matrix. After this, their substrates were carefully ground and polished to $A'_{S1} \approx 52 \mu\text{m}$, $A'_{S2} \approx 206 \mu\text{m}$, and $A'_{S3} \approx 346 \mu\text{m}$ individually using an abrasive machine. A Photonetic 3642CR00 tunable laser with a single-mode fiber pigtail was adopted as the light source. Before performing measurements, the optical path was well collimated to ensure that the laser exiting from the fiber pigtail was illuminated vertically onto the EG-FPF. Finally, the transmission spectra of the three EG-FPFs were obtained within the wavelength range of 1545–1565 nm as shown in Figs. 5(b)–(d). As predicted, the transmission side peaks are gradually suppressed along with the decrease in substrate thickness. The side peaks are distributed roughly symmetrically around the main peaks (Figs. 5(c) and (d)), which ensures that A'_{S2} and A'_{S3} are in the range expressed by Eq. (8). Furthermore, the PT in Fig. 5(b) shows the same level as those shown in Figs. 5(c) and (d), guaranteeing that A'_{S1} also stays within the range expressed by Eq. (8). However, the PTs shown in

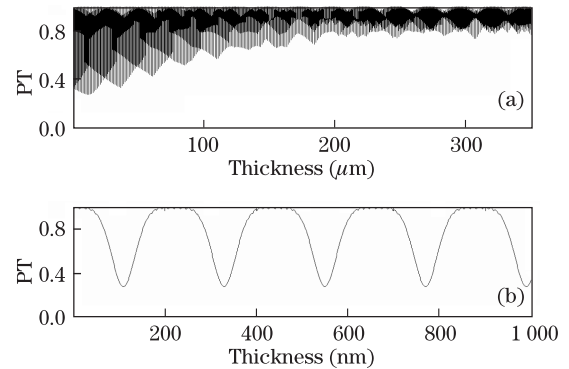


Fig. 4. Simulated PT around 1550 nm of the EG-FPF as a function of substrate thickness (a) from 0 to $350 \mu\text{m}$ and (b) from 0 to 1000 nm.

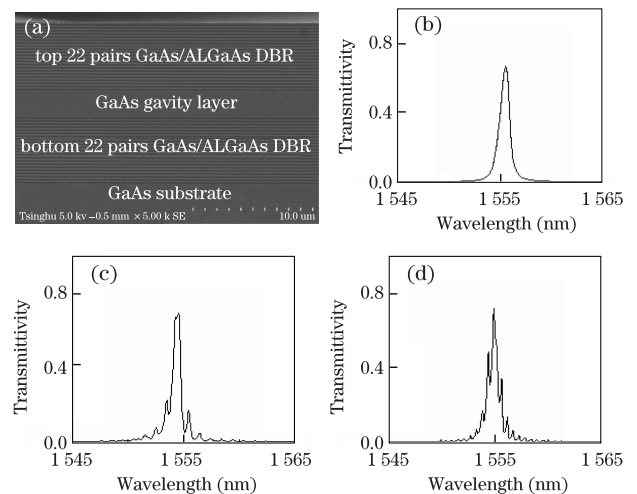


Fig. 5. (a) Cross-sectional SEM image of the EG-FPF and the measured transmission spectra with the substrates (b) A'_{S1} , (c) A'_{S2} , and (d) A'_{S3} ground, respectively.

Figs. 5(b)-(d) are only about 70%, much lower than 1, a result attributed mainly to the loss of scattering and absorption caused by the defects of the EG-FPF. Additionally, the transmission peaks shift from the theoretical value of 1550 nm to the practical value of around 1555 nm because of the deviation of the growing process in MOCVD.

In conclusion, we investigate the influence of GaAs substrate on the transmission performance of an EG-FPF. With increasing substrate thickness, the resonant transmission peak of the EG-FPF begins to deteriorate by splitting because of the periodic modulation of the substrate. Moreover, rapid oscillation of the PT, along with the alteration of substrate thickness, is theoretically obtained. To realize an acceptable transmission spectrum by suppressing the side peaks, we suggest that the substrate be thinned down to a suitable thickness range through well-controlled grinding and polishing. This approach is implemented experimentally.

This work was supported by the National "973" Program of China (No. 2010CB327600), the National "863" Program of China (No. 2007AA03Z418), the Program for Changjiang Scholars and Innovative Research Team in University (No. IRT0609), the Fundamental Research Funds for the Central University (No. BUPT2011RC0403), the National Natural Science Foundation of China (No. 61020106007), and the "111" Project of China (No. B07005).

References

1. M. V. Kotlyar, L. O'Faolain, A. B. Krysa, and T. F. Krauss, *J. Lightwave Technol.* **23**, 2169 (2005).
2. H. Gao, S. Yuan, L. Bo, G. Li, J. Zhang, G. Kai, and X. Dong, *J. Lightwave Technol.* **26**, 2282 (2008).
3. D. Hays, A. Zribi, S. Chandrasekaran, S. Goravar, S. Maity, L. R. Douglas, K. Hsu, and A. Banerjee, *J. Microelectromech. Syst.* **19**, 419 (2010).
4. W. Ren, P. Tao, Z. Tan, Y. Liu, and S. Jian, *Chin. Opt. Lett.* **7**, 775 (2009).
5. H. Kim, J. Joo, J. Choi, B. Jun, and C. Kim, *IEEE Trans. Appl. Supercond.* **15**, 2767 (2005).
6. S. P. Tobin, S. M. Vernon, C. Bajgar, S. J. Wojtczuk, M. R. Melloch, A. Keshavarzi, T. B. Stellwag, S. Venkatesan, M. S. Lundstrom, and K. A. Emery, *IEEE Trans. Electron. Dev.* **37**, 469 (1990).
7. P. Li, L. Wang, S. Li, W. Xia, X. Zhang, Q. Tang, Z. Ren, and X. Xu, *Chin. Opt. Lett.* **7**, 489 (2009).
8. H. Huang, Y. Huang, and X. Ren, *Electron. Lett.* **39**, 113 (2003).
9. X. Duan, Y. Huang, H. Huang, X. Ren, Q. Wang, Y. Shang, X. Ye, and S. Cai, *J. Lightwave Technol.* **27**, 4697 (2009).
10. X. Duan, Y. Huang, Q. Wang, H. Huang, X. Ren, and K. Wen, *Chinese J. Lasers (in Chinese)* **36**, 2362 (2009).
11. X. F. Duan, Y. Huang, X. Ren, H. Huang, S. Xie, Q. Wang, and S. Cai, *Opt. Express* **18**, 5879 (2010).
12. C. Hums, T. Finger, T. Hempel, J. Christen, and A. Dadgar, *J. Appl. Phys.* **101**, 033113 (2007).
13. M. J. Mondry, D. I. Babit, J. E. Bowers, and L. A. Coldren, *IEEE Photon. Technol. Lett.* **4**, 627 (1992).
14. T. Makino, *J. Lightwave Technol.* **12**, 2092 (1994).
15. S. Jiang, L. Dong, R. Zhang, and S. Xie, *Chin. Opt. Lett.* **7**, 960 (2009).